

The Relationship Between the Uncinate Fasciculus and Anxious Temperament Is Evolutionarily Conserved and Sexually Dimorphic

Do P.M. Tromp, Andrew S. Fox, Jonathan A. Oler, Andrew L. Alexander, and Ned H. Kalin

ABSTRACT

BACKGROUND: Anxious temperament (AT) is an early-life heritable trait that predisposes individuals to develop anxiety and depressive disorders. Our previous work in preadolescent children suggests alterations in the uncinate fasciculus (UF), the white matter tract that connects prefrontal with limbic regions, in boys with anxiety disorders. Here, using a nonhuman primate model of AT, we tested whether this sexually dimorphic finding is evolutionarily conserved and examined the extent to which heritable and environmental influences contribute to UF microstructure.

METHODS: Diffusion tensor images were collected in 581 young rhesus monkeys (1.89 ± 0.77 years old; 43.9% female). Using tract-based analyses, we assessed the relationship among AT, UF microstructure (as measured with fractional anisotropy), and sex. Heritability of tract microstructure was determined using oligogenic linkage analysis of this large multigenerational pedigree.

RESULTS: We predicted and found a negative relation between AT and UF fractional anisotropy in male but not female monkeys (AT \times sex; $p = .032$, 1-tailed). Additionally, heritability analyses revealed that variation in UF fractional anisotropy was largely due to nonheritable factors ($h^2 = 0.185$, $p = .077$).

CONCLUSIONS: These results demonstrate a cross-species, male-specific relation between UF microstructure and anxiety and provide a potential substrate for anxiety-related prefrontal-limbic dysregulation. The heritability analyses point to the importance of environmental influences on UF microstructure, which could be important in mediating the nonheritable components of pathological anxiety. These findings have the potential to guide new treatment strategies for childhood anxiety disorders and further support the use of nonhuman primates as a translational model to discover mechanisms underlying the development of anxiety.

Keywords: Anxiety, Anxious temperament, DTI, Nonhuman primates, Sex differences, White matter

<https://doi.org/10.1016/j.biopsych.2019.07.022>

Anxiety disorders are among the most prevalent psychiatric disorders, and worldwide it is estimated that ~25% of individuals will experience one or more anxiety disorders in their lifetime (1). The likelihood of developing an anxiety disorder increases through a combination of genetic and environmental factors. For example, having a parent with an anxiety disorder confers increased risk that is likely mediated by heritability and social learning. Estimates for the heritability of anxiety disorders vary between 20% and 40% (2–6). Anxiety disorders frequently begin in childhood (7), and considerable research has demonstrated the ability to detect an early-life anxious phenotype that is associated with a 3- to 4-fold increased risk to develop anxiety and mood disorders (8,9). This phenotype, termed behavioral inhibition or the related anxious temperament (AT), is evolutionarily conserved across nonhuman primates and humans (10). Understanding the environmental and genetic factors that influence the neural mechanisms underlying AT has the potential to aid in conceptualizing novel early-life intervention strategies.

Children with high levels of behavioral inhibition, similar to young monkeys with extreme AT, display heightened

behavioral and physiological reactivity to threat (10–13), responses that are thought to be mediated by the amygdala via projections to its downstream targets (14,15). Nonhuman primate studies demonstrate that increased amygdala metabolism is associated with AT (16–18), a finding that is consistent with studies of individuals with a history of behavioral inhibition as well as individuals with anxiety disorders (19–21). Additionally, in both nonhuman primates and humans, reduced functional coupling between the amygdala and regulatory regions such as the prefrontal cortex (PFC) is associated with AT and anxiety disorders (22–25).

The uncinate fasciculus (UF) is of interest because it is a key white matter structure that is involved in frontolimbic connectivity (26–28). Research in both adults and children has implicated the UF as a pathway that is altered in anxiety disorders (29–34). Specifically, adults with anxiety disorders display significantly reduced UF fractional anisotropy (FA), a measure of white matter microstructure (29–34). Our previous study in preadolescent children with anxiety disorders more directly links these findings to pathophysiological mechanisms, because the reduced UF FA cannot be attributed to illness

chronicity and/or psychotropic medication exposure (35). Importantly, the reduction in UF FA associated with anxiety disorders appears to be sexually dimorphic, such that it was observed in boys and not girls (35). Further studies elaborating the factors underlying this effect in male subjects will be important in understanding sex-specific pathophysiologies and in deriving novel treatment targets.

The rhesus monkey is ideally suited to uncover mechanisms relevant to human pathological anxiety because of similarities between humans and rhesus monkeys in brain structure and function and in social and emotional behavior (13,36,37). Like humans, the rhesus monkey has a well-developed PFC, with similar connectivity between the amygdala and the PFC conveyed by the UF (13). Therefore, we developed and validated a reliable nonhuman primate model of AT focused on understanding the early risk to develop anxiety and other stress-related psychopathology. With this model, using a large fully phenotyped multigenerational pedigree, we defined the neural circuit that underlies AT (16,17,38). We also found that AT was approximately 29% heritable (17), which is similar to the heritability observed in human anxiety and anxiety disorders (2–6), and that metabolism in components of the AT circuit are also significantly heritable (17).

We now use this large sample to understand whether the reduction in UF FA observed in boys with anxiety disorders is evolutionarily conserved, and if so, the extent to which it is influenced by heritable and nonheritable factors. More specifically, we explore the hypothesis that AT is related to UF FA, and as in human children, that this effect is sexually dimorphic and selectively occurring in male monkeys. In addition to the UF, we explore the heritability of microstructure in other prominent white matter tracts. These data set the stage for mechanistic and proof-of-concept nonhuman primate studies with the ultimate aim of developing new early-life circuit-based interventions.

METHODS AND MATERIALS

Subjects

Behavioral, endocrine, and neuroimaging assessments were performed in 594 young rhesus monkeys (*Macaca mulatta*); of these, 581 animals (326 male, 255 female) had usable diffusion imaging data and were included in this study. The average age was 1.89 ± 0.77 years, with a range between 0.84 and 4.42 years (Supplemental Figure S1). This age in monkeys is roughly equivalent to prepubescent children between 3 and 12 years old. Imaging data from some of these subjects was previously published (16–18,24,39). All 581 animals were from a large multigenerational pedigree of 1928 animals (805 male, 1123 female) across 9 generations (0th–8th). The relations of the animals for which diffusion imaging data was collected can be traced back 1 to 8 generations, with most animals being in the 4th to 6th generations (see Supplemental Figure S2). For additional details, see our previous publications (16,17,40). Procedures were performed using protocols approved by the University of Wisconsin Institutional Animal Care and Use Committee.

Behavioral Assessment

Rhesus monkeys were exposed to a human intruder paradigm to assess behavioral and endocrine responses to a mild threat.

Blood samples were collected to measure plasma cortisol levels post exposure. To create the composite measure of AT, an average of the z scores of freezing, inverse cooing, and cortisol was computed for each subject. For additional details see the Supplement.

Endocrine Assessment

Details of the endocrine assessment are reported in the Supplement.

Neuroimaging Assessment

Magnetic Resonance Imaging Acquisition. To investigate white matter microstructure, magnetic resonance imaging scans were collected within 4 months of the No-Eye-Contact exposure. Data were collected at 2 imaging locations using GE SIGNA 750 3.0T scanners (General Electric, Waukesha, WI) and a transmit-receive quadrature extremity coil (Invivo Corp, Gainesville, FL). Details of the scan sequence are reported in the Supplement. Briefly, the animals were anesthetized and placed in a stereotactic frame inside the magnetic resonance imaging coil. T1-weighted anatomical images were collected in addition to diffusion-weighted images and their corresponding field map. A change in the scan sequence was implemented midway through the study, and this was accounted for by covarying for this variable in the analyses.

Diffusion Tensor Imaging Analyses. Details of the diffusion tensor imaging (DTI) analyses are reported in the Supplement, and processing steps as well as code can be found online (<http://www.diffusion-imaging.com>). Briefly, white matter microstructure was characterized by using the diffusion-weighted imaging volumes to calculate the local diffusion tensor in each voxel (Figure 1A). Diffusion-weighted imaging volumes were distortion corrected, tensors were estimated, and images were normalized to a population template and warped to our previously published 592-rhesus monkey T1-template (<http://www.pnas.org/content/112/29/9118>; Supplementary Dataset S01) with a 0.625-mm isotropic resolution. The mean population template, created from all subjects, was used for deterministic fiber tractography to delineate tracts of interest (Figure 1B, C). Whole-brain fiber tractography was performed, and white matter pathways were iteratively delineated using anatomically defined waypoints (41,42) (see Figure 1C for the waypoints used in UF extraction). Tracts extracted included corpus callosum, cingulum bundle, internal capsule, inferior fronto-occipital fasciculus, stria terminalis and fornix, and UF. Owing to limited DTI resolution and close proximity of the stria terminalis and fornix, the two pathways were combined. Because we had no a priori hypothesis about left- versus right-tract differences, the bilateral components of each tract were combined into one average. Multiple diffusion measures beyond FA were estimated to characterize and quantify the microstructural tissue properties of each tract, including mean diffusivity, axial diffusivity, and radial diffusivity.

Heritability Analyses

Heritability was estimated based on pedigree information using SOLAR Eclipse software package (43) (http://www.nitrc.org/projects/se_linux). Quantitative genetic analysis partitions

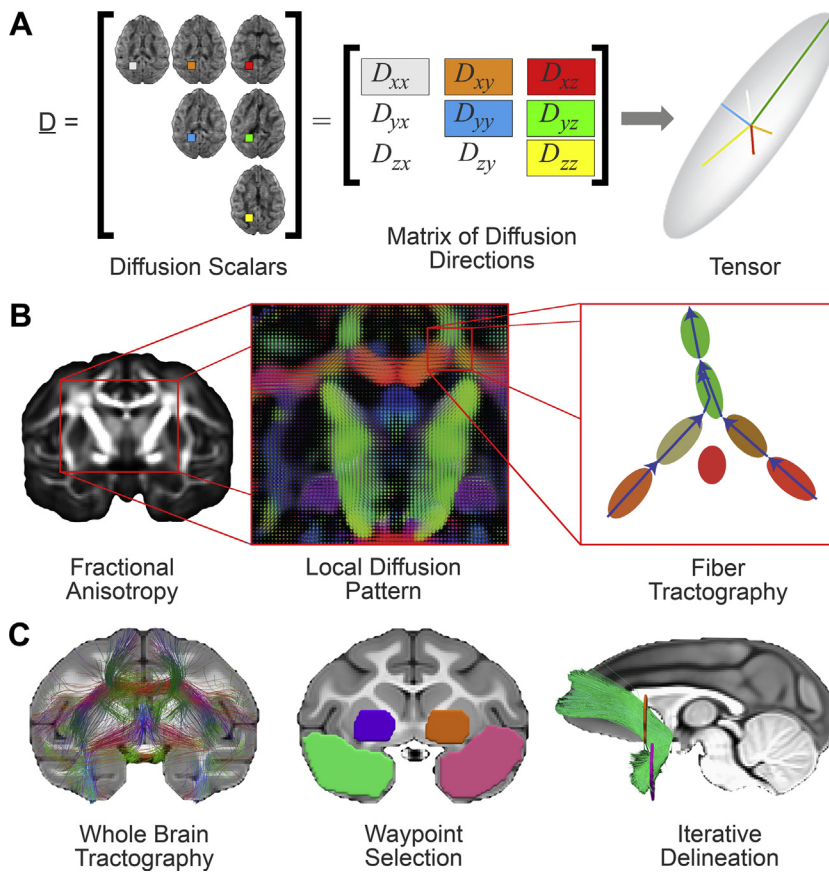


Figure 1. Diffusion tensor imaging methods. Overview of methods used for diffusion tensor imaging processing and analysis. **(A)** The scanner collects a scalar image of water diffusion throughout the brain at multiple noncollinear directions. Combining the amount of water diffusion with the applied matrix of diffusion directions provides a diffusion tensor for each voxel in the brain. **(B)** Local brain microstructure is quantified by using diffusion measures such as fractional anisotropy, where bright regions represent highly anisotropic tensors and dark regions indicate more isotropic tensors, indicating an underlying microstructure with high and low levels of white matter fibers, respectively. Next, fiber tractography can be applied to follow the direction of each tensor to get an estimate of the underlying white matter anatomy. **(C)** After running fiber tractography throughout the whole brain, waypoint selection can be used to delineate fiber tracts of interest using anatomically defined waypoints. Iterative delineation must be used to minimize the inclusion of spurious tracts.

the observed covariance among related individuals into genetic versus environmental components. The additive genetic variance, heritability (h^2), was estimated by employing a maximum likelihood variance decomposition-based method. For a pedigree of animals, the covariance matrix Ω is given by

$$\Omega = 2 \cdot \Phi \cdot \sigma_g^2 + I \cdot \sigma_e^2$$

where Ω is the covariance matrix of the phenotype, Φ is the kinship matrix for the pedigree, σ_g^2 is the variance in the trait due to additive genetic effects, I is the identity matrix, and σ_e^2 is the variance due to unmeasured random environmental effects. Variance parameters are estimated by comparing the covariance due to phenotype matrix with the covariance due to kinship matrix (43). Significance is tested by comparing the model where σ_g^2 is constrained to 0, to a model where σ_g^2 is estimated. The log likelihood ratio was calculated as twice the difference between these models. Under the null hypothesis, the test statistic is distributed as a 50:50 mixture of a χ^2 variate with 1 degree of freedom and a point mass at 0. Heritability was estimated for each behavior and white matter tract for the full group and within male and female monkeys separately. To ensure that these traits conform to the assumptions of normality, an inverse normal transformation was applied.

We also tested the difference in heritability between UF and the other extracted pathways. This was accomplished by

comparing a model where the 2 heritability estimates of these pairwise tracts were allowed to vary independently with a model that constrained the heritability estimates to be equal. Furthermore, we estimated the shared heritability between mean tract FA and AT by running a bivariate heritability analysis, where $\rho = 0$. For more details on the heritability estimation methods see previous publications (17,43).

Statistical Analyses

All statistical analyses were run with robust linear regression models to mitigate the effect of outliers on the results. Sex differences in age, weight, behavior, and cortisol were calculated. The significance of the interaction between AT and sex on tract microstructure was calculated. All analyses were controlled for age, sex, site, scanner properties, number of No-Eye-Contact exposures, and test order. Next, within-sex analyses were run to determine the relation between AT and tract microstructure within the male and female monkeys separately. Owing to our a priori hypothesis on the direction of these effects, a negative relation between UF FA and AT in male but not female monkeys, the AT by sex interaction on UF FA, and the within-sex regression between AT and UF FA in male monkeys were tested 1-tailed. All other statistical tests were 2-tailed. For the tracts with no a priori predictions, we applied a Šidák familywise error correction ($\alpha_{SID} = 1 - [1 - \alpha]^{1/m}$), where m is the number of tracts, which in

Table 1. Demographic Information

	Female	Male	<i>p</i> Value
Sample Size	255	326	n.a.
Age, Years	1.95 (0.82)	1.80 (0.70)	.028 ^a
Weight, kg	3.20 (1.19)	3.18 (1.08)	.528
AT	−0.05 (0.66)	0.02 (0.66)	.195
Cortisol, µg/dL	0.26 (17.61)	1.80 (16.24)	.286
Coo Vocalizations	2.25 (2.91)	2.23 (2.70)	.883
Freezing	1.41 (1.43)	1.57 (1.42)	.084

Demographic, behavioral, and cortisol data and significance of sex differences are displayed for female and male rhesus monkeys. Values are presented as *n* or mean (SD). Statistics for AT and its components used transformed and residualized data.

AT, anxious temperament; n.a., not applicable.

^a*p* < .05.

this case is 5. Models were run using the statsmodels package in Python (44).

Heritability analyses were run in SOLAR and controlled for age, age-squared, sex, and the age by sex interaction. When the analyses were run within sex, the covariates included age and age-squared. SOLAR output included the heritability value (h^2), significance (*p*), and the standard error.

RESULTS

AT in Female and Male Monkeys

Male and female monkeys did not differ in their expression of AT ($p = .195$) (Table 1); however, freezing levels tended to be higher in male compared with female monkeys ($z_{579} = 1.726$, $p = .084$) (Table 1). Other AT constituents such as coo vocalizations and cortisol levels, as well as weight, did not significantly differ between male and female monkeys ($p > .28$) (Table 1). On average, male monkeys were slightly younger than the female monkeys ($z_{579} = -2.197$, $p = .028$) (Table 1).

Assessment of UF FA in Relation to AT

Using the methods described, we characterized the UF in our population of rhesus monkeys. As can be seen in Figure 2, this tract is highly similar to that we previously characterized in preadolescent children (35). Based on our previous work, we predicted that UF FA would be negatively related to AT in male but not in female monkeys (35). Results demonstrated this predicted effect. Specifically, we found an interaction between AT and sex on UF FA that was averaged across right and left tracts ($z_{570} = -1.861$, $p = .032$, 1-tailed) (Figure 3, Supplemental Table S2). We also analyzed UF FA from each hemisphere individually, which resulted in similar findings (Supplemental Table S3). Similar to our findings in humans, analyses in the male monkeys revealed a significant negative relation between UF FA and AT ($z_{317} = -1.794$, $p = .037$, 1-tailed) (Figure 3, Supplemental Table S2). Consistent with the interaction being driven by the male monkeys, no significant relation between UF FA and AT was observed in female monkeys ($z_{246} = 1.288$, $p = .198$; 2-tailed) (Figure 3, Supplemental Table S2). Additionally, there was not a significant main effect for the relation between UF FA and AT across

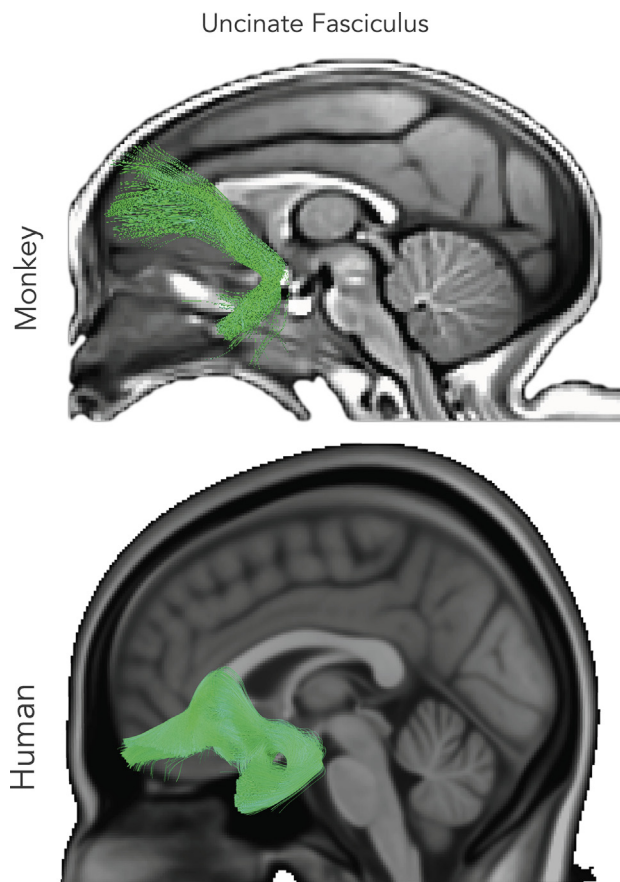


Figure 2. Comparison of uncinate fasciculus across species. Depicted is a comparison of the uncinate fasciculus in humans and monkeys. This qualitative comparison indicates largely evolutionarily conserved white matter architecture. The human image is modified from a previously published image in our study of preadolescent children with anxiety disorders (35).

male and female monkeys ($p = .326$, 2-tailed) (Supplemental Table S2).

Follow-up analyses examined whether the individual components of AT (freezing, cooing, cortisol) were also related to UF FA. Similar to the UF-AT relation, we found a significant sex by freezing interaction ($z_{570} = -2.465$, $p = .007$, 1-tailed) (Supplemental Table S4) and a significant sex by coo vocalizations interaction ($z_{570} = 1.826$, $p = .034$, 1-tailed) (Supplemental Table S4) on UF FA. However, we did not observe a sex by cortisol interaction on UF FA ($z_{570} = 0.599$, $p = .275$, 1-tailed) (Supplemental Table S4). The anxiety-related effects were specific to UF FA, as none of the other tracts or other diffusion measures (mean diffusivity, axial diffusivity, or radial diffusivity) demonstrated main effects or sex interactions (see Supplemental Tables S2 and S5). As was observed in the UF, the other tracts are largely homologous to equivalent human tracts (Supplemental Figure S3).

We tested main effects and interactions for age, sex, and AT on UF FA. While UF FA was significantly negatively affected by age ($z_{567} = -2.103$, $p = .035$) (Supplemental Table S4), the rate of UF FA change did not significantly differ between sexes

Relation Between Uncinate Fasciculus and Anxiety in Monkeys

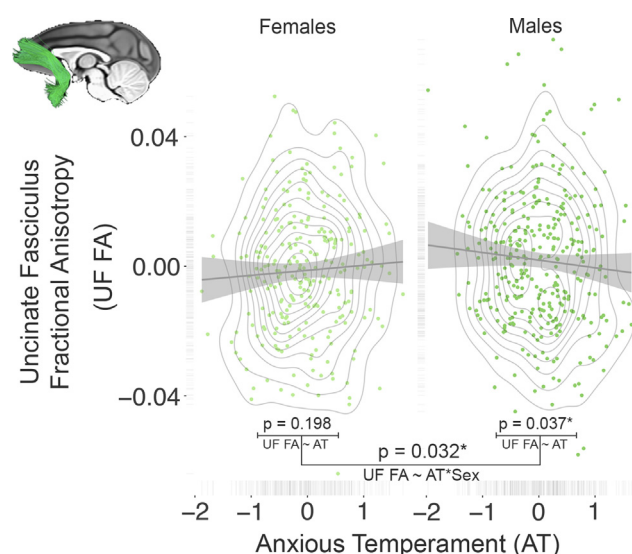


Figure 3. Uncinate fasciculus (UF) fractional anisotropy (FA) and anxious temperament (AT). When testing the interaction between AT and sex on UF FA, results indicate a 1-tailed significant interaction ($p = .032$, 1-tailed), such that male monkeys (right; dark green) display a negative relation between AT and UF FA ($p = .037$, 1-tailed), but female monkeys (left; light green) do not ($p = .198$, 2-tailed). The scatterplots display linear regression lines with confidence intervals, density estimation contours, and rug plots of the marginal distributions for AT and UF FA values. Plotted values for UF FA are residualized for the covariates.

($p = .618$) (Supplemental Table S4). Additionally, there were no significant AT by sex by age interactions ($p = 0.413$) (Supplemental Table S4).

Heritability

Because of interest in the genetic and environmental factors that mediate anxiety, we used our large multigenerational pedigree to perform analyses estimating the heritability of AT, its components, and tract microstructure. Our previous work demonstrated AT to be significantly heritable in a larger sample that included the animals in this study (17). We first verified that these findings held across male and female monkeys for whom we had DTI data ($h^2 = 0.292$, $p < .001$) (Table 2). Because we identified sex differences in the UF-AT relation, we separately examined the heritability of AT in the male and female monkeys. We found higher heritability estimates in the female compared with the male monkeys; however, the 95% confidence intervals (CIs) for these heritability estimates were overlapping (female: h^2 95% CI = -0.02 to 0.89 ; male: h^2 95% CI = -0.00 to 0.58) (Supplemental Table S6). We also found that the AT's components (coo vocalizations, cortisol, and freezing) were significantly heritable ($p < .025$) (Supplemental Table S6).

Because of the relation between AT and UF FA, we performed an analysis examining the heritability of UF FA. Across male and female monkeys the results indicated low heritability for UF FA ($h^2 = 0.185$, $p = .077$) (Table 2), as well as low heritability when analyzing the male and female monkeys separately (female: $h^2 = 0$, $p = .5$; male: $h^2 = 0.236$, $p = .12$) (Table 2). These results indicate that the majority of the variance in UF FA

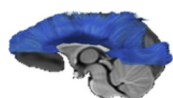
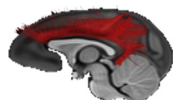
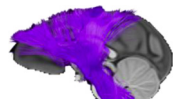
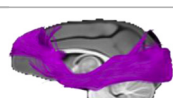

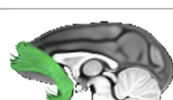
can be explained by nonheritable factors. To determine whether this was specific to the UF or whether this was more general of white matter during this developmental period, we examined the heritability of FA within 5 additional tracts (corpus callosum, cingulum bundle, internal capsule, inferior fronto-occipital fasciculus, and stria terminalis/fornix). Interestingly, in contrast to the UF, FA in all of the other extracted tracts demonstrated significant heritability ($p < .005$) (Table 2). Tests comparing the heritability of UF FA with the other tracts confirmed that UF FA heritability was significantly less than that in the corpus callosum ($\chi^2 = 5.66$, $p = .017$) (Supplemental Table S7) and the inferior fronto-occipital fasciculus ($\chi^2 = 6.41$, $p = .011$) (Supplemental Table S7). Even though UF FA was not significantly heritable, we explored the possibility that UF FA would demonstrate coheritability with AT. Not surprisingly, we found that UF FA was not significantly coheritable with AT; FA in the other white matter tracts examined was also not coheritable with AT (see Supplemental Table S8 for an overview in the full sample). Consistent with largely nonheritable variation in UF, heritability analyses of other UF diffusivity measures (mean diffusivity, axial diffusivity, and radial diffusivity) were not significant (see Supplemental Table S9 for details, as well as data across all the other tracts).

DISCUSSION

Early-life anxious temperament is a risk factor for the later development of anxiety and depressive disorders. Our previous work in young children with anxiety disorders demonstrated a sex-specific decrease in UF FA in young boys with anxiety disorders, which was not seen in young girls (35). Here, using our well-validated rhesus monkey model of AT, we focused on the relation between AT and white matter microstructure in the UF. The UF is important because it is the major white matter pathway connecting prefrontal with limbic regions and likely plays a role in mediating the transfer of information relevant to adaptive and maladaptive emotion regulation (26,27). The current results demonstrate a sexually dimorphic relation between UF FA and AT, such that in young male monkeys higher levels of AT are associated with lower UF FA values. These findings extend our work in anxious young children and suggest an evolutionarily conserved relationship between UF microstructure and early-life anxiety in boys but not girls (35).

We emphasize that prefrontal-limbic dysregulation is thought to contribute to pathological anxiety in both male and female individuals. The current data point to a potential mechanism in male monkeys that does not appear to be present in female monkeys. It is conceivable that there are multiple pathways that can result in prefrontal-limbic dysregulation. For example, dysregulation could result from overactivity of the amygdala, decreased input to the amygdala from orbital frontal cortex, or altered function of other prefrontal regions involved in cognition and emotion regulation, such as the dorsolateral prefrontal cortex. While a few studies in the literature have adequate sample sizes to confidently examine sex differences, most studies addressing these issues are underpowered. More clearly understanding mechanisms in male and female individuals that underlie prefrontal-amygdala regulation is an important question for future research.

Table 2. Heritability Analyses of FA

Heritability		All Monkeys (N = 581)		Female (n = 255)		Male (n = 326)	
		h^2 (SE)	p Value	h^2 (SE)	p Value	h^2 (SE)	p Value
Tract FA							
CC		0.57 (0.121)	<.001 ^a	0.504 (0.207)	.004 ^a	0.735 (0.179)	<.001 ^a
CING		0.346 (0.112)	<.001 ^a	0.345 (0.183)	.017 ^b	0.325 (0.142)	.002 ^a
IC		0.227 (0.082)	<.001 ^a	0.364 (0.179)	.007 ^a	0.284 (0.133)	.004 ^a
IFO		0.496 (0.116)	<.001 ^a	0.443 (0.198)	.007 ^a	0.554 (0.178)	<.001 ^a
STRIA/FX		0.322 (0.129)	.001 ^a	0.418 (0.234)	.021 ^b	0.187 (0.151)	.073
UF		0.185 (0.142)	.077	0	.500	0.236 (0.22)	.120

Heritability (mean h^2 , SE, and p values) are presented here for FA in each white matter tract, for all monkeys, and for female and male monkeys separately.

CC, corpus callosum; CING, cingulum bundle; FA, fractional anisotropy; IC, internal capsule; IFO, inferior fronto-occipital fasciculus; STRIA/FX, striatum and fornix; UF, uncinate fasciculus.

^aSidak-corrected significance at $p < .0085$.

^bUncorrected significance at $p < .05$.

The observed relation between AT and white matter microstructure is specific to UF FA, as no other white matter tracts or other measures of white matter integrity were related to AT. Variation in FA can be attributed to genetic and/or environmental factors. Importantly, in the current study, we found that in the preadolescent to early adult age range studied, individual differences in UF FA appear to be largely determined by nonheritable factors. These results point to the importance of early-life environmental influences in determining white matter microstructure that is relevant to prefrontal-limbic function as it relates to the expression of AT. While we did not find heritability to be a significant determinant of UF FA at this age, it is possible that heritability could play a greater role as individuals mature. This is supported by observations in human twin studies suggesting low levels of UF FA heritability at 9 years of age that increase into adulthood (45–47).

Regardless of the factors that determine individual differences in UF FA, the FA measurement can reflect variation in fiber organization, axonal density, and/or myelination. All of these features of white matter microstructure can be important in determining the speed, timing, and accuracy of neural

signals. In relation to our findings, which point to the importance of environment in determining variation in UF FA, evidence from animal and human studies suggests that white matter pathways can be dynamically altered in response to learning and other experiences (48–50). Imaging studies in animals and humans demonstrate increased FA associated with learning and skill acquisition (49). At a histological level, animal studies demonstrate activity-dependent increases in myelin basic protein (51,52). It is thought that a fundamental component of activity-dependent changes in white matter occurs via signaling at the “axo-myelinic” synapse, which is the interface between immature and mature oligodendrocytes with the axonal membrane (53).

Our finding of the relation between UF FA and AT in male monkeys leads to the question of what mechanisms might play a role in this sexually dimorphic effect. Because heritability can be affected by sex, we examined this possibility. However, we did not find substantial sex differences in the estimated heritability of UF FA. It is also unlikely that adolescent-related influences of sex hormones on brain maturation (54) are relevant to this finding, as our monkeys were primarily prepubertal. In this regard, we note that there were no main effects of sex on

Relation Between Uncinate Fasciculus and Anxiety in Monkeys

UF FA, and no sex by age interactions. The lack of heritable effects points to the importance of environmental influences on establishing the male-specific relation between UF FA and AT. Because this finding is consistent across humans and nonhuman primates, it is possible that sex-related differences in rearing and/or socialization that are conserved across species could be important. Rhesus monkey mothers have been observed to treat their infant male and female offspring differently. For example, mothers display more embrace and approach behaviors toward their female infants (55, 56) and exhibit more mutual gazing with their male infants (57). Furthermore, studies across human and nonhuman species consistently demonstrate sex-related behavioral differences that are manifested early in life, and it is possible that these differences in behavior affect white matter development. For example, studies in rhesus monkeys have demonstrated sex-related differences in social play in which male infants initiate play more frequently and exhibit more rough-and-tumble play (58), while female infants engage in more approach-avoidance play (59). It is possible that the sex-related differences that we observed between anxiety and white matter microstructure could in part be due to sex-related behavioral differences occurring during periods of heightened white matter neuroplasticity. It is also important to recognize that rodent studies reveal male-female differences in the regulation of oligodendrocytes (60). Female rodents have a higher turnover rate of oligodendrocytes, as characterized by increased proliferation and increased apoptosis (61,62). Other data implicate testosterone in facilitating white matter repair in experimentally lesioned animals (63).

While the findings of this study are consistent with findings in children with anxiety disorders, we note the current study's limitations. Although we studied a large sample of rhesus monkeys, the age distribution was predominantly limited to preadolescent animals. Thus, it is possible that the observed effect could be age related. Additionally, we did not collect data relevant to the early rearing environment, which precludes our ability to specifically examine the role of environmental events. Finally, we note that the scanning resolution used in this study may have obscured other effects on white matter microstructure.

Our results in young nonhuman primates provide a cross-species confirmation for a male-specific role of the UF in anxiety-related prefrontal-limbic dysregulation. The findings further support the translational relevance of the nonhuman primate AT model. Because we observed that the majority of UF FA variance is due to nonheritable factors, and research is indicating that myelination is dynamic and activity dependent throughout life, this opens the door for studying myelin changes in relation to current effective interventions as well as thinking about the development of new treatments. The hypothesis would be that enhanced UF FA would facilitate more efficient communication between the PFC and critical limbic structures, resulting in adaptive anxiety regulation. Based on the activity-dependent nature of myelin plasticity and the role of the UF FA in prefrontal-limbic regulation, it will be important to assess the extent to which changes in UF FA are associated with individual differences in treatment outcomes. We expect that current interventions thought to work by modifying prefrontal-limbic interactions, such as exposure therapy,

cognitive behavioral therapy, and transcranial magnetic stimulation, would increase UF FA. By using UF FA as a dependent measure, these therapies could be optimized in relation to their intensity, frequency of administration, and length of time over which the intervention is used.

The value of the nonhuman primate model is to explore the molecular mechanisms that mediate these effects on promoting myelin plasticity. Clues could be provided by assessing differences in UF oligodendrocyte gene regulation between monkeys with high- and low-anxiety levels as they relate to microstructural integrity. Identifying the genes that are the most predictive of UF FA will provide insights into molecular targets that could be leveraged to promote UF FA plasticity. Once identified, nonhuman primate models can be used to examine the extent to which the identified genes are causally related to UF FA and AT, as well as to effective treatment strategies.

It is likely that strategies that selectively activate anxiety-regulating neural circuitry between PFC and limbic regions could be of benefit. Additionally, efforts to optimize our treatments such that they promote increases in UF FA will be of value. For example, this could be achieved by intensive training over time in relation to the mastery of anxiety-related amygdala responses. While current treatments such as exposure therapy involve the acquisition of mastery techniques, the exact parameters necessary to optimally influence white matter are yet unclear. However, evidence suggests that healthful and stress-reducing activities such as aerobic exercise, sleep, and environmental enrichment positively impact white matter (49,64). New treatments could be conceptualized that combine strategies that enhance myelination in tracts, such as the UF, with interventions aimed at activating and "training" key brain regions involved in anxiety regulation that are connected by the UF. For example, we predict that increased UF FA could be achieved by repetitive and consistent exposure to anxiety-provoking, limbic-activating stimuli, in conjunction with mastery training of induced anxiety. Future studies will be important to establish how these early-life male-specific relations between UF FA and AT can inform the development of new sex-specific treatment strategies for anxiety disorders.

ACKNOWLEDGMENTS AND DISCLOSURES

This work was supported by grants from the National Institutes of Health (Grant Nos. R01-MH046729, R01-MH081884, P50-MH084051 and P50-MH100031 [to NHH]; P51-OD011106 and P51-RR000167 [to the Wisconsin National Primate Research Center]; and P30-HD003352 [to the Waisman Center]).

We thank H. van Valkenberg, P.H. Roseboom, M.A. Jesson (University of Wisconsin-Madison), J. Rogers (Baylor College of Medicine), J. Blangero (University of Texas-Rio Grande Valley) and the staffs of the Harlow Center for Biological Psychology, Lane Neuroimaging Laboratory at the Health-Emotions Research Institute, Waisman Laboratory for Brain Imaging and Behavior, and Wisconsin National Primate Research Center.

ALA is part owner of Thervoyant. At the time of writing, NHH had received honoraria from CME Outfitters, Elsevier, and the Pritzker Consortium; served on scientific advisory boards for Actify Neurotherapies and Neuronetics; serves as an advisor to the Pritzker Neuroscience Consortium; consults to Concept Therapeutics; served as co-editor of *Psychoneuroendocrinology*; serves as editor-in-chief of *The American Journal of Psychiatry*; and has patents on promoter sequences for corticotropin-releasing factor CRF2 α and a method of identifying agents that alter the activity of the promoter sequences (Patent Nos. 7,071,323 and 7,531,356), promoter

sequences for urocortin II and the use thereof (Patent No. 7,087,385), and promoter sequences for corticotropin-releasing factor binding protein and the use thereof (Patent No. 7,122,650). The other authors report no biomedical financial interests or potential conflicts of interest.

ARTICLE INFORMATION

From the Department of Psychiatry (DPMT, JAO, ALA, NHK), Neuroscience Training Program (DPMT, NHK), HealthEmotion Research Institute (DPMT, JAO, NHK), and Department of Medical Physics (ALA), University of Wisconsin, Madison, Wisconsin; and Department of Psychology (ASF) and California National Primate Research Center (ASF), University of California, Davis, California.

Address correspondence to Ned Kalin, M.D., HealthEmotion Research Institute, Department of Psychiatry, 6001 Research Park Boulevard, Madison, WI 53719; E-mail: nkalin@wisc.edu.

Received Jan 17, 2019; revised Jul 6, 2019; accepted Jul 23, 2019.

Supplementary material cited in this article is available online at <https://doi.org/10.1016/j.biopsych.2019.07.022>.

REFERENCES

- Kessler RC, Petukhova M, Sampson NA, Zaslavsky AM, Wittchen H-U (2012): Twelve-month and lifetime prevalence and lifetime morbid risk of anxiety and mood disorders in the United States. *Int J Methods Psychiatr Res* 21:169–184.
- Hettema JM, Neale MC, Kendler KS (2001): A review and meta-analysis of the genetic epidemiology of anxiety disorders. *Am J Psychiatry* 158:1568–1578.
- Jardine R, Martin NG, Henderson AS, Rao DC (1984): Genetic covariation between neuroticism and the symptoms of anxiety and depression. *Genet Epidemiol* 1:89–107.
- Martin N, Goodwin G, Fairburn C, Wilson R, Allison D, Cardon LR, Flint J (2000): A population-based study of personality in 34,000 sib-pairs. *Twin Res* 3:310–315.
- Calboli FCF, Tozzi F, Galwey NW, Antoniadou A, Mooser V, Preisig M, et al. (2010): A genome-wide association study of neuroticism in a population-based sample. *PLoS One* 5:e11504.
- Bouchard TJ, Loehlin JC (2001): Genes, evolution, and personality. *Behav Genet* 31:243–273.
- Kessler RC, Ruscio AM, Shear K, Wittchen H-U (2010): Epidemiology of anxiety disorders. *Curr Top Behav Neurosci* 2:21–35.
- Fox NA, Henderson HA, Marshall PJ, Nichols KE, Ghera MM (2005): Behavioral inhibition: Linking biology and behavior within a developmental framework. *Annu Rev Psychol* 56:235–262.
- Clauss JA, Blackford JU (2012): Behavioral inhibition and risk for developing social anxiety disorder: A meta-analytic study. *J Am Acad Child Adolesc Psychiatry* 51:1066–1075.
- Kalin N, Shelton S (1989): Defensive behaviors in infant rhesus monkeys: Environmental cues and neurochemical regulation. *Science* 243:1718–1721.
- Kagan J (1997): Temperament and the reactions to unfamiliarity. *Child Dev* 68:139–143.
- Craske MG, Rauch SL, Ursano R, Prenoveau J, Pine DS, Zinbarg RE (2009): What is an anxiety disorder? *Depress Anxiety* 26:1066–1085.
- Kalin NH, Shelton SE (2003): Nonhuman primate models to study anxiety, emotion regulation, and psychopathology. *Ann N Y Acad Sci* 1008:189–200.
- Alheid GF, Heimer L (1988): New perspectives in basal forebrain organization of special relevance for neuropsychiatric disorders: The striatopallidum, amygdaloid, and corticopetal components of substantia innominata. *Neuroscience* 27:1–39.
- Bandler R, Shipley MT (1994): Columnar organization in the midbrain periaqueductal gray: Modules for emotional expression? *Trends Neurosci* 17:379–389.
- Oler JA, Fox AS, Shelton SE, Rogers J, Dyer TD, Davidson RJ, et al. (2010): Amygdalar and hippocampal substrates of anxious temperament differ in their heritability. *Nature* 466:864–868.
- Fox AS, Oler JA, Shackman AJ, Shelton SE, Raveendran M, McKay DR, et al. (2015): Intergenerational neural mediators of early-life anxious temperament. *Proc Natl Acad Sci U S A* 112:9118–9122.
- Fox AS, Shelton SE, Oakes TR, Davidson RJ, Kalin NH (2008): Trait-like brain activity during adolescence predicts anxious temperament in primates. *PLoS One* 3:e2570.
- Etkin A, Wager TD (2007): Functional neuroimaging of anxiety: A meta-analysis of emotional processing in PTSD, social anxiety disorder, and specific phobia. *Am J Psychiatry* 164:1476–1488.
- Holzschnieder K, Mulert C (2011): Neuroimaging in anxiety disorders. *Dialogues Clin Neurosci* 13:453–461.
- Martin EI, Ressler KJ, Binder E, Nemeroff CB (2010): The neurobiology of anxiety disorders: Brain imaging, genetics, and psychoneuroendocrinology. *Clin Lab Med* 30:865–891.
- Etkin A, Prater KE, Hoeft F, Menon V, Schatzberg AF (2010): Failure of anterior cingulate activation and connectivity with the amygdala during implicit regulation of emotional processing in generalized anxiety disorder. *Am J Psychiatry* 167:545–554.
- Hahn A, Stein P, Windischberger C, Weissenbacher A, Spindelegger C, Moser E, et al. (2011): Reduced resting-state functional connectivity between amygdala and orbitofrontal cortex in social anxiety disorder. *Neuroimage* 56:881–889.
- Bim RM, Shackman AJ, Oler JA, Williams LE, McFarlin DR, Rogers GM, et al. (2014): Evolutionarily conserved prefrontal-amygdalar dysfunction in early-life anxiety. *Mol Psychiatry* 19:915–922.
- Monk CS, Telzer EH, Mogg K, Bradley BP, Mai X, Louro HMC, et al. (2008): Amygdala and ventrolateral prefrontal cortex activation to masked angry faces in children and adolescents with generalized anxiety disorder. *Arch Gen Psychiatry* 65:568–576.
- Schmahmann JD, Pandya DN, Wang R, Dai G, D'Arceuil HE, de Crespigny AJ, Wedeen VJ (2007): Association fibre pathways of the brain: Parallel observations from diffusion spectrum imaging and autoradiography. *Brain* 130:630–653.
- Catani M, Howard RJ, Pajevic S, Jones DK (2002): Virtual in vivo interactive dissection of white matter fasciculi in the human brain. *Neuroimage* 17:77–94.
- Rudebeck PH, Saunders RC, Prescott AT, Chau LS, Murray EA (2013): Prefrontal mechanisms of behavioral flexibility, emotion regulation and value updating. *Nat Neurosci* 16:1140–1145.
- Tromp DPM, Grupe DW, Oathes DJ, McFarlin DR, Hernandez PJ, Kral TR, et al. (2012): Reduced structural connectivity of a major frontolimbic pathway in generalized anxiety disorder. *Arch Gen Psychiatry* 69:925–934.
- Phan KL, Orlichenko A, Boyd E, Angstadt M, Coccaro EF, Liberzon I, Arfanakis K (2009): Preliminary evidence of white matter abnormality in the uncinate fasciculus in generalized social anxiety disorder. *Biol Psychiatry* 66:691–694.
- Baur V, Brühl AB, Herwig U, Eberle T, Rufer M, Delsignore A, et al. (2013): Evidence of frontotemporal structural hypoconnectivity in social anxiety disorder: A quantitative fiber tractography study. *Hum Brain Mapp* 34:437–446.
- Hettema JM, Kettenmann B, Ahluwalia V, McCarthy C, Kates WR, Schmitt JE, et al. (2012): Pilot multimodal twin imaging study of generalized anxiety disorder. *Depress Anxiety* 29:202–209.
- Baur V, Hänggi J, Rufer M, Delsignore A, Jäncke L, Herwig U, Beatrix Brühl A (2011): White matter alterations in social anxiety disorder. *J Psychiatr Res* 45:1366–1372.
- Liao M, Yang F, Zhang Y, He Z, Su L, Li L (2014): White matter abnormalities in adolescents with generalized anxiety disorder: a diffusion tensor imaging study. *BMC Psychiatry* 14:41.
- Tromp DPM, Williams LE, Fox AS, Oler JA, Roseboom PH, Rogers GM, et al. (2019): Altered uncinate fasciculus microstructure in childhood anxiety disorders in boys but not girls. *Am J Psychiatry* 176:208–216.
- Belmonte JCI, Callaway EM, Churchland P, Caddick SJ, Feng G, Homanics GE, et al. (2015): Brains, genes, and primates. *Neuron* 86:617–631.
- Oishi K, Huang H, Yoshioka T, Ying SH, Zee DS, Zilles K, et al. (2011): Superficially located white matter structures commonly seen in the

Relation Between Uncinate Fasciculus and Anxiety in Monkeys

- human and the macaque brain with diffusion tensor imaging. *Brain Connect* 1:37–47.
38. Kalin NH, Shelton SE, Fox AS, Oakes TR, Davidson RJ (2005): Brain regions associated with the expression and contextual regulation of anxiety in primates. *Biol Psychiatry* 58:796–804.
 39. Adluru N, Zhang H, Fox AS, Shelton SE, Ennis CM, Bartosic AM, *et al.* (2012): A diffusion tensor brain template for rhesus macaques. *Neuroimage* 59:306–318.
 40. Rogers J, Shelton SE, Shelledy W, Garcia R, Kalin NH (2008): Genetic influences on behavioral inhibition and anxiety in juvenile rhesus macaques. *Genes Brain Behav* 7:463–469.
 41. Mori S, Kaufmann WE, Davatzikos C, Stieltjes B, Amodei L, Fredericksen K, *et al.* (2002): Imaging cortical association tracts in the human brain using diffusion-tensor-based axonal tracking. *Magn Reson Med* 223:215–223.
 42. Tromp D (2016): DTI tutorial 3–Fiber tractography. *Winrower* 6. e146228.88526.
 43. Almasy L, Blangero J (1998): Multipoint quantitative-trait linkage analysis in general pedigrees. *Am J Hum Genet* 62:1198–1211.
 44. Seabold S, Perktold J (2010): Statsmodels: Econometric and statistical modeling with Python. In: der Walt S, Millman J, editors. *Proceedings of the 9th Python in Science Conference*. Austin, Texas: SciPy 2010, 57–61.
 45. Brouwer RM, Mandl RCW, Peper JS, van Baal GCM, Kahn RS, Boomsma DI, Hulshoff Pol HE (2010): Heritability of DTI and MTR in nine-year-old children. *Neuroimage* 53:1085–1092.
 46. Brouwer RM, Mandl RC, Schnack HG, van Soelen IL, van Baal GC, Peper JS, *et al.* (2012): White matter development in early puberty: A longitudinal volumetric and diffusion tensor imaging twin study. *PLoS One* 7:e32316.
 47. Budisavljevic S, Kawadler JM, Dell'Acqua F, Rijdsdijk FV, Kane F, Picchioni M, *et al.* (2016): Heritability of the limbic networks. *Soc Cogn Affect Neurosci* 11:746–757.
 48. Gibson EM, Purger D, Mount CW, Goldstein AK, Lin GL, Wood LS, *et al.* (2014): Neuronal activity promotes oligodendrogenesis and adaptive myelination in the mammalian brain. *Science* 344:1252304.
 49. Sampaio-Baptista C, Johansen-Berg H (2017): White matter plasticity in the adult brain. *Neuron* 96:1239–1251.
 50. Fields RD, Dutta DJ (2019): Treadmilling model for plasticity of the myelin sheath. *Trends Neurosci* 42:443–447.
 51. Sampaio-Baptista C, Khrapitchev AA, Foxley S, Schlagheck T, Scholz J, Jbabdi S, *et al.* (2013): Motor skill learning induces changes in white matter microstructure and myelination. *J Neurosci* 33:19499–19503.
 52. Blumenfeld-Katzir T, Pasternak O, Dagan M, Assaf Y (2011): Diffusion MRI of structural brain plasticity induced by a learning and memory task. *PLoS One* 6:e20678.
 53. Micu I, Plemel JR, Capriarello AV, Nave KA, Stys PK (2018): Axo-myelinic neurotransmission: A novel mode of cell signalling in the central nervous system. *Nat Rev Neurosci* 19:49–58.
 54. Perrin JS, Hervé P-Y, Leonard G, Perron M, Pike GB, Pitiot A, *et al.* (2008): Growth of white matter in the adolescent brain: Role of testosterone and androgen receptor. *J Neurosci* 28:9519–9524.
 55. Mitchell GD (1968): Attachment differences in male and female infant monkeys. *Child Dev* 39:611–620.
 56. Kulik L, Langos D, Widdig A (2016): Mothers make a difference: Mothers develop weaker bonds with immature sons than daughters. *PLoS One* 11:e0154845.
 57. Dettmer AM, Kaburu SSK, Byers KL, Murphy AM, Soneson E, Wooddell LJ, Suomi SJ (2016): First-time rhesus monkey mothers, and mothers of sons, preferentially engage in face-to-face interactions with their infants. *Am J Primatol* 78:238–246.
 58. Brown GR, Dixon AF (2000): The development of behavioural sex differences in infant rhesus macaques (*Macaca mulatta*). *Primates* 41:63–77.
 59. Meaney MJ, Stewart J, Beatty WW (1985): Sex differences in social play: The socialization of sex roles. *Adv Study Behav* 15:2–58.
 60. Swamydas M, Bessert D, Skoff R (2009): Sexual dimorphism of oligodendrocytes is mediated by differential regulation of signaling pathways. *J Neurosci Res* 87:3306–3319.
 61. Cerghet M, Skoff RP, Swamydas M, Bessert D (2009): Sexual dimorphism in the white matter of rodents. *J Neurol Sci* 286:76–80.
 62. Cerghet M, Skoff RP, Bessert D, Zhang Z, Mullins C, Ghandour MS (2006): Proliferation and death of oligodendrocytes and myelin proteins are differentially regulated in male and female rodents. *J Neurosci* 26:1439–1447.
 63. Hussain R, Ghomari AM, Bielecki B, Steibel J, Boehm N, Liere P, *et al.* (2013): The neural androgen receptor: A therapeutic target for myelin repair in chronic demyelination. *Brain* 136:132–146.
 64. Hughes EG, Orthmann-Murphy JL, Langseth AJ, Bergles DE (2018): Myelin remodeling through experience-dependent oligodendrogenesis in the adult somatosensory cortex. *Nat Neurosci* 21:696–706.

The Relationship Between the Uncinate Fasciculus and Anxious Temperament Is Evolutionarily Conserved and Sexually Dimorphic

Supplemental Information

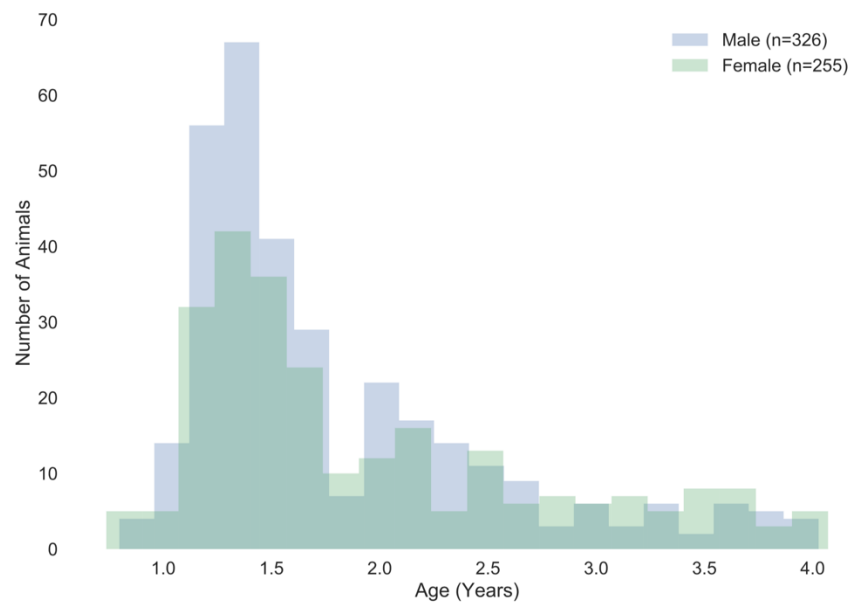


Figure S1. Age of subjects. Histogram of age distribution for male (blue) and female (green) rhesus monkeys included in the study.

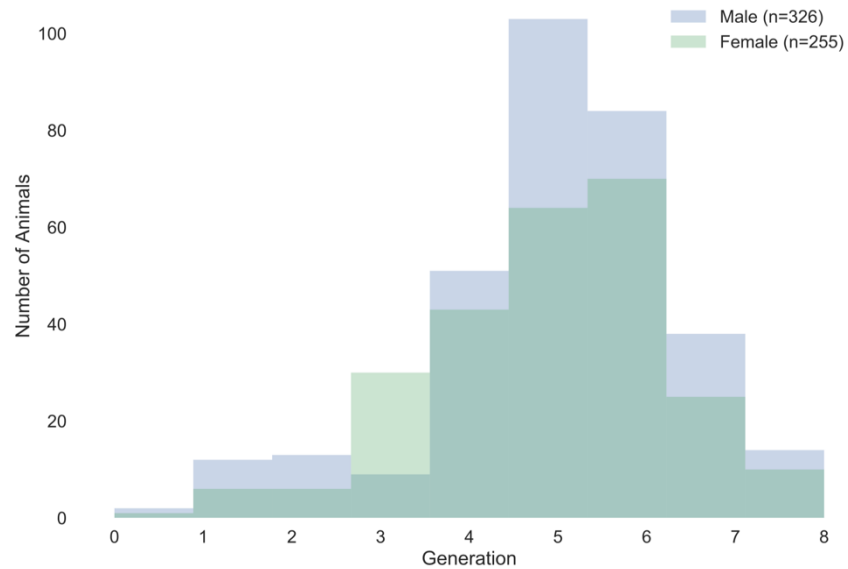


Figure S2. Distribution of phenotyped subjects across generations. Histogram depicting the distribution of male (blue) and female (green) rhesus monkeys by generation.

Table S1. Behavioral coding details. Description of behavioral coding for coo vocalizations and freezing.

Behavior	Description
Coo Vocalizations	Vocalization made by rounding and pursing the lips with an increase then decrease in frequency and intensity. <i>Frequency of behavior is coded.</i>
Freezing	A period of at least three seconds characterized by tense body posture, no vocalizations and no movement other than slow movements of the head. If animal vocalizes freezing is not rated at the same time. Duration of behavior is coded.

Supplemental Methods

Behavioral Assessment Continued

Rhesus monkeys were exposed to a human intruder paradigm to assess behavioral and endocrine responses to a mild threat. In this human intruder paradigm the animals were exposed to the No-Eye-Contact (NEC) condition for 30 minutes (1). During this exposure the animals are placed in a test-cage, after which a human “intruder” enters the room and displays the profile of their face to the animal for 30 minutes at 2.5 meters distance, while making no eye contact. Blood samples were collected to measure plasma cortisol levels post exposure.

During the NEC condition behaviors were observed and assessed by trained raters using a closed circuit television system (1). Behaviors were assessed according to the definitions found in supplementary Table S1. All behaviors were log-transformed when the duration of the behavior was quantified, and root transformed when the frequency was quantified (as previously described (2, 3)). To create the composite measure of AT, an average of the z-scores of freezing, inverse cooing and cortisol was computed for each subject.

Endocrine Assessment Continued

Cortisol levels were assessed from blood (plasma; 7 ml EDTA tube) after exposure to a mild stressor (NEC). Bloods were drawn between 8am-1pm for 82% of the sample. Collection occurred while the animal was under sedation with ketamine (15 mg/kg, IM). Plasma was immediately separated from whole blood by centrifugation at 4°C and frozen

at -70°C until assayed. Cortisol was measured by radioimmunoassay using the DPC Coat-a-count assay following the manufacturer's instructions (Siemens, Los Angeles, CA). Samples were diluted 8-fold prior to being measured in duplicate, and samples that had a CV% > 20 were repeated. Linear effects for time of day were removed from the cortisol values. This was performed by using the beta-weights for each time point that were derived from the linear regression between time of day and cortisol across subjects.

Neuroimaging Assessment

MRI acquisitions continued

The animals received ketamine (15 mg/kg, IM) prior to the scan. The animal was then placed in the sphinx position using a custom stereotactic frame that fit inside the MRI coil, while heart rate and oxygen saturation were monitored. Administration of ketamine (up to 5 mg/kg, IM) was repeated as needed to maintain anesthesia, approximately every 20-40 minutes throughout the scan. At the end of the scan the animals were removed from the scanner and monitored until they fully recovered from anesthesia.

Anatomical images were acquired to help mask brain from skull. Axial T1-weighted 3D inversion recovery prepared fast spoiled gradient recalled scan (IR-fSPGR) were collected with these parameters; repetition time (TR) = 8.64 ms, echo time (TE) = 1.89 ms, inversion time (TI) = 600 ms, flip angle $\alpha = 10^{\circ}$, number of excitations (NEX) = 2, field of view (FOV) = 140 mm, matrix = 256x224, scanner interpolated spatial sampling = 0.27x0.27x0.5 mm.

Diffusion-weighted imaging (DWI) scans were collected with a corresponding field map to correct for field inhomogeneities, which are stronger in monkeys compared to

humans when scanned on conventional MRI scanners. A change in scan sequence was implemented during the course of the study. All DWIs were collected using a two-dimensional, echo-planar, spin-echo sequence. For the first 313 individuals, DWI scans were collected with the following parameters: TR = 10 s; TE = 77.2 ms; FOV = 140 mm; matrix = 128×128 (interpolated to 256×256 on the scanner); 2.5mm thick contiguous slices; echo-planar echo spacing = 800 μ s. Diffusion-weighted imaging ($b = 1000 \text{ s/mm}^2$) was performed in 12 non-collinear directions with one non-diffusion weighted image, the acquisition was repeated six times and averaged on the scanner. For the next 268 subjects DWI scans were collected with the following parameters: TR = 6.1 s; TE = 90.1 ms; FOV = 140 mm; matrix = 128×128 (interpolated to 256×256 on the scanner); 2.5 mm thick contiguous slices; echo-planar echo spacing = 932 μ s. Diffusion-weighted imaging ($b = 1000 \text{ s/mm}^2$) was performed in 72 non-collinear directions with 6 non-diffusion weighted images. For both sequences a co-planar field map was also obtained using a gradient echo with images at two echo times: TE₁ = 7 ms, TE₂ = 10 ms.

DTI analyses continued

White matter microstructure was characterized by using the DWI volumes to calculate the local diffusion tensor in each voxel (Figure 1A). First, DWI volumes were corrected for movement and eddy current distortions using FMRIB Software Library (FSL) tools for affine registration. To correct the gradient directions after volume registration, the b-matrix was adjusted for the applied registrations parameters (4). Field inhomogeneities were corrected by applying the skull stripped co-planar field map using in-house code. T1-scans were registered to the field maps so that the manually skull-stripped T1-masks

could be warped and applied to the field map for optimal field correction results and which produced a corrected DWI image without skull.

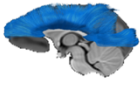
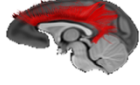



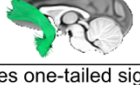
Next, tensors were estimated. The influence of local artifacts on the tensor calculation was reduced by using a method for robust estimation of tensors by outlier rejection (RESTORE, as implemented in Camino software (5)). To allow for cross subject comparisons all subjects were normalized to template space. Tensor images were transformed to an population template space using the diffusion tensor imaging toolkit's (DTI-TK) nonlinear normalization tools (6), which iteratively construct a template from the tensor files using a tensor based registration. The final population template was then aligned to our previously published 592 rhesus monkey T1-template (<http://www.pnas.org/content/112/29/9118>; Supplementary Dataset S01) with a 0.625 mm isotropic resolution. This warp was then applied to all normalized images, so that the final tensor file for each subject was registered to 592-space.

The mean population template in 592-space, created from all subjects, was used for deterministic fiber tractography to delineate tracts of interest (Figure 1B/C). In the rhesus monkeys, similar to our previous human work (7), whole-brain fiber tractography was performed using Camino software (5), that implemented a tensor deflection (TEND) algorithm for optimal estimation of the fiber tracking directions (8, 9) (Figure 1B). Fiber tracking was terminated in voxels where FA was below 0.1 or where the angle between consecutive streamline steps was more than 90 degrees. Visualization software TrackVis (10) was used to iteratively delineate white matter pathways using anatomically defined waypoints (11, 12) (See Figure 1C for the waypoints used in UF extraction). Tracts extracted included: corpus callosum (CC), cingulum bundle (CING), internal capsule (IC),

inferior fronto-occipital fasciculus (IFO), stria terminalis/fornix (STRIA/FX) and UF. Due to limited DTI resolution and close proximity of the STRIA and FX, the two pathways were combined. Since we had no *a priori* hypothesis about left versus right tract differences, the bilateral components of each tract were combined into one average.

Multiple diffusion measures beyond FA were estimated to characterize and quantify the microstructural tissue properties of each tract. FA is a normalized variance measure of directional diffusivities and is highest in regions with highly organized, dense white matter fiber pathways. Mean diffusivity (MD) is a directionally-averaged measure of water diffusion and is sensitive to the density of tissue membranes and microstructure. Axial diffusivity (AD) and radial diffusivity (RD) reflect diffusion properties in the parallel and perpendicular directions, respectively, relative to the white matter tracts (for an overview (13)). A weighted-mean for each diffusion measure (FA, MD, AD, RD) was calculated for each tract. This approach assigns relatively more weight to values in voxels that have a higher fiber count (14), which is most frequently observed in areas more central to the white matter tract of interest. In theory this method should reduce the influence of voxels that are on tissue boundaries and often suffer from partial volume effects (15).

Table S2. Tract-based analyses of FA. White matter tract means (\pm standard deviation) and regression statistics (z-values) for AT, as well as the interaction of AT by Sex on tract FA, for all subjects, as well as in females and males separately. All effects are reported two-tailed; p-values presented in brackets are one-tailed due to a priori hypotheses.

Tract FA		All Subjects (n = 581)				Females (n = 255)			Males (n = 326)		
		mean (SD)	Tract FA ~ AT		* Sex	mean (SD)	Tract FA ~ AT		mean (SD)	Tract FA ~ AT	
			z-values	p-values	p-values		z-values	p-values		z-values	p-values
CC		0.346 (0.028)	1.205	0.228	0.516	0.343 (0.029)	1.044	0.297	0.348 (0.027)	0.18	0.857
CING		0.269 (0.024)	0.686	0.493	0.708	0.267 (0.024)	0.259	0.796	0.271 (0.023)	-0.195	0.845
IC		0.372 (0.021)	0.169	0.866	0.62	0.372 (0.020)	-0.129	0.897	0.372 (0.021)	0.947	0.344
IFO		0.342 (0.018)	0.011	0.991	0.834	0.341 (0.019)	-0.184	0.854	0.342 (0.018)	-0.358	0.72
STRIA /FX		0.230 (0.012)	0.125	0.901	0.891	0.227 (0.012)	-0.319	0.749	0.231 (0.012)	0.192	0.848
UF		0.206 (0.022)	0.983	0.326	0.063 [0.032]*	0.204 (0.022)	1.288	0.198	0.208 (0.023)	-1.794	0.073 [0.037]*

* indicates one-tailed significant at $p < 0.05$, ** indicates sidak corrected significance at $p < 0.01$. Abbreviations: Anxious Temperament (AT), Corpus Callosum (CC), Cingulum bundle (CING), Fractional Anisotropy (FA), Internal Capsule (IC), Inferior Fronto-Occipital fasciculus (IFO), Stria Terminalis & Fornix (STRIA/FX), Uncinate Fasciculus (UF).

Table S3. Tract-based analyses of left and right UF FA. Uncinate fasciculus means (\pm standard deviation) and regression statistics (z-values) for AT, as well as the interaction of AT by Sex on tract FA, for all subjects, as well as in females and males separately. All effects are reported two-tailed; p-values presented in brackets are one-tailed due to a priori hypotheses.

Tract FA	All Subjects (n = 581)			Females (n = 255)		Males (n = 326)	
	Tract FA ~ AT		* Sex	Tract FA ~ AT		Tract FA ~ AT	
	z-values	p-values	p-values	z-values	p-values	z-values	p-values
UF Right	0.941	0.347	0.095 [0.047]*	1.341	0.180	-1.536	0.125 [0.063]
UF Left	0.784	0.433	0.067 [0.034]*	0.941	0.347	-1.923	0.054 [0.027]*


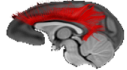
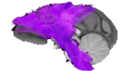

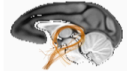
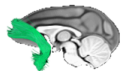
* indicates one-tailed significant at $p < 0.05$, ** indicates sidak corrected significance at $p < 0.01$. Abbreviations: Anxious Temperament (AT), Fractional Anisotropy (FA), Uncinate Fasciculus (UF).

Table S4. Additional analyses. Top: Significance (p-values) for the regression of the individual AT components cooing, cortisol and freezing, and their interaction with sex on UF FA. Bottom: Significance (p-values) of the three way interaction between AT, Sex and Age, as well as all two way interactions and main effects on UF FA. All effects are reported two-tailed, p-values in brackets are one-tailed due to *a priori* hypotheses. Analyses include covariates as reported in the methods.

Dependent Variable	All Subjects			
	UF FA ~ X + X * Sex (+ Covariates)			
(df = 570)	Main Effect	X*Sex		
X = Cortisol	0.094	0.549 [0.275]		
X = Coo Vocalizations	0.114	0.068 [0.034]*		
X = Freezing	0.08	0.014 [0.007]**		
Dependent Variable	UF FA ~ AT + Sex + Age + (AT*Sex) + (AT*Age) + (Sex*Age) + (AT*Sex*Age) (+ Covariates)			
(df = 567)	Main Effect	AT*X	Sex*X	AT*Sex*X
X = AT	0.276			
X = Sex	0.393	0.053 [0.027]*		
X = Age	0.035**	0.257	0.618	0.413

* indicates one-tailed significant at $p < 0.05$. ** indicates two-tailed significant at $p < 0.05$.

Table S5. Tract-based analyses of MD, AD & RD. White matter tract means (\pm standard deviation) and regression statistics (z-values) for AT, as well as the interaction of AT by Sex on tract MD, AD or RD, for all subjects. All effects are reported two-tailed.

Tract MD, AD & RD	All Subjects				All Subjects				All Subjects			
	mean MD (SD)	Tract MD ~ AT		* Sex	mean AD (SD)	Tract AD ~ AT		* Sex	mean RD (SD)	Tract RD ~ AT		* Sex
		z-values	p-values	p-values		z-values	p-values	p-values		z-values	p-values	p-values
CC 	0.681 (0.043)	-0.093	0.926	0.8	0.960 (0.051)	0.476	0.634	0.719	0.542 (0.043)	-0.447	0.655	0.854
CING 	0.740 (0.034)	0.181	0.857	0.595	0.956 (0.035)	0.823	0.411	0.753	0.631 (0.037)	0.013	0.989	0.697
IC 	0.654 (0.037)	-1.155	0.248	0.253	0.945 (0.046)	-1.119	0.263	0.21	0.508 (0.035)	-1.081	0.28	0.35
IFO 	0.700 (0.031)	-0.073	0.942	0.864	0.982 (0.040)	-0.145	0.884	0.826	0.559 (0.030)	-0.055	0.956	0.97
STRIA /FX 	0.725 (0.078)	-0.339	0.734	0.932	0.914 (0.092)	-0.395	0.693	1	0.631 (0.072)	-0.313	0.755	0.898
UF 	0.692 (0.094)	0.254	0.8	0.31	0.850 (0.119)	0.381	0.703	0.17	0.613 (0.082)	0.171	0.864	0.446

* indicates one-tailed significant at $p < 0.05$, ** indicates sidak corrected significance at $p < 0.01$. Abbreviations: Axial Diffusivity (AD), Anxious Temperament (AT), Corpus Callosum (CC), Cingulum bundle (CING), Internal Capsule (IC), Inferior Fronto-Occipital fasciculus (IFO), Mean Diffusivity (MD), Radial Diffusivity (RD), Stria Terminalis & Fornix (STRIA/FX), Uncinate Fasciculus (UF).

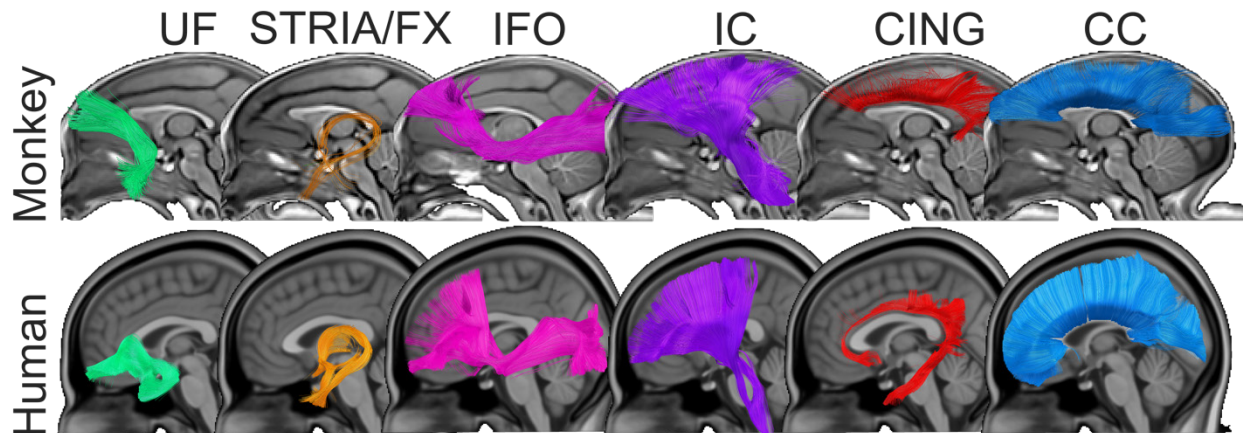


Figure S3. Comparison of tracts across species. Depicted is a comparison of white matter tracts in humans and monkeys. This qualitative comparison indicates largely evolutionarily conserved white matter architecture. The human images are modified from a previously published image in our study of preadolescent children with anxiety disorders (7).

Table S6. Heritability analyses of AT. Heritability (mean and standard error) and its significance are presented here for AT and its components, for all subjects, as well as females and males separately.

Heritability	All Subjects (n = 581)		Females (n = 255)		Males (n = 326)	
	H ² (SE)	p-values	H ² (SE)	p-values	H ² (SE)	p-values
AT	0.292 (0.096)	<0.001*	0.433 (0.233)	0.014*	0.29 (0.147)	0.007*
Cortisol	0.139 (0.086)	0.021*	0	0.500	0.184 (0.122)	0.034*
Coo Vocalizations	0.277 (0.098)	<0.001*	0.301 (0.187)	0.034*	0.223 (0.158)	0.046*
Freezing	0.338 (0.111)	<0.001*	0.287 (0.215)	0.065	0.251 (0.163)	0.038*

* indicates significance at $p < 0.05$. Abbreviations: Anxious Temperament (AT), Standard Error (SE).

Table S7. Tract heritability differences.

Significance of the pairwise comparison of models where heritability of FA in CC, CING, IC, IFO and STRIA/FX were constrained to be equal to the heritability of UF FA, and unconstrained models.

Heritability Comparison	All Subjects	
	Chi ²	<i>p</i> -values
UF FA:		
CC FA	5.66	0.017*
CING FA	0.73	0.393
IC FA	0.46	0.496
IFO FA	6.41	0.011*
STRIA/FX FA	0.25	0.616

* indicates significance at $p < 0.05$.

Abbreviations: Corpus Callosum (CC), Cingulum bundle (CING), Fractional Anisotropy (FA), Internal Capsule (IC), Inferior Fronto-Occipital fasciculus (IFO), Stria Terminalis & Fornix (STRIA/FX), Uncinate Fasciculus (UF).

Table S8. Shared heritability. Genetic correlation between AT and the FA for each of the white matter tracts that were extracted.

Co-heritability	All Subjects	
	Rho _g	<i>p</i> -values
AT:		
CC FA	0.15	0.440
CING FA	-0.13	0.628
IC FA	-0.06	0.824
IFO FA	-0.23	0.260
STRIA/FX FA	-0.12	0.655
UF FA	-0.03	0.917

* indicates significance at $p < 0.05$.

Abbreviations: Anxious Temperament (AT), Corpus Callosum (CC), Cingulum bundle (CING), Fractional Anisotropy (FA), Internal Capsule (IC), Inferior Fronto-Occipital fasciculus (IFO), Stria Terminalis & Fornix (STRIA/FX), Uncinate Fasciculus (UF).

Table S9. Heritability analyses of MD, AD & RD. Heritability (mean and standard error) and its significance are presented here for MD, AD & RD in each white matter tract, for all subjects, and for females and males separately.

Heritability	All Subjects (n = 581)		Females (n = 255)		Males (n = 326)	
	H ² (SE)	p-values	H ² (SE)	p-values	H ² (SE)	p-values
Tract MD:						
CC	0.135 (0.108)	0.086	0.093 (0.188)	0.304	0.271 (0.268)	0.175
CING	0 (0)	0.500	0 (0)	0.500	0.406 (0.209)	0.017*
IC	0.087 (0.077)	0.092	0 (0)	0.500	0.432 (0.181)	0.001*
IFO	0 (0)	0.500	0 (0)	0.500	0.119 (0.241)	0.309
STRIA/FX	0.198 (0.096)	0.010*	0 (0)	0.500	0.203 (0.18)	0.108
UF	0 (0)	0.500	0 (0)	0.500	0 (0)	0.500
Tract AD:						
CC	0.302 (0.12)	0.002*	0.312 (0.22)	0.072	0.578 (0.253)	0.008*
CING	0.158 (0.097)	0.030*	0.109 (0.221)	0.307	0.68 (0.207)	<0.001*
IC	0.095 (0.085)	0.094	0 (0)	0.500	0.383 (0.181)	0.005*
IFO	0.025 (0.09)	0.387	0 (0)	0.500	0.301 (0.227)	0.078
STRIA/FX	0.234 (0.1)	0.003*	0 (0)	0.500	0.261 (0.189)	0.062
UF	0 (0)	0.500	0 (0)	0.500	0 (0)	0.500
Tract RD:						
CC	0.163 (0.099)	0.027*	0.102 (0.166)	0.257	0.319 (0.219)	0.060
CING	0.055 (0.088)	0.254	0.036 (0.181)	0.420	0 (0)	0.500
IC	0.197 (0.085)	0.001*	0.132 (0.159)	0.185	0.36 (0.153)	0.001*
IFO	0.027 (0.083)	0.371	0 (0)	0.500	0 (0)	0.500
STRIA/FX	0.19 (0.11)	0.022*	0.008 (0.173)	0.482	0.089 (0.178)	0.299
UF	0 (0)	0.500	0 (0)	0.500	0 (0)	0.500

* indicates significance at $p < 0.05$. Abbreviations: Axial Diffusivity (AD), Corpus Callosum (CC), Cingulum bundle (CING), Internal Capsule (IC), Inferior Fronto-Occipital fasciculus (IFO), Mean Diffusivity (MD), Radial Diffusivity (RD), Standard Error of the Mean (SEM), Stria Terminalis & Fornix (STRIA/FX), Uncinate Fasciculus (UF).

Supplementary References

1. Kalin N, Shelton S (1989): Defensive behaviors in infant rhesus monkeys: environmental cues and neurochemical regulation. *Science* (80-). 243: 1718–1721.
2. Oler J a, Fox AS, Shelton SE, Rogers J, Dyer TD, Davidson RJ, *et al.* (2010): Amygdalar and hippocampal substrates of anxious temperament differ in their heritability. *Nature*. 466: 864–8.
3. Fox AS, Shelton SE, Oakes TR, Davidson RJ, Kalin NH (2008): Trait-like brain activity during adolescence predicts anxious temperament in primates. *PLoS One*. 3: e2570.
4. Leemans A, Jones DK (2009): The B-matrix must be rotated when correcting for subject motion in DTI data. *Magn Reson Med*. 61: 1336–1349.
5. Cook PA, Bai Y, Seunarine KK, Hall MG, Parker GJ, Alexander DC (2006): Camino : Open-Source Diffusion-MRI Reconstruction and Processing. 14: 22858.
6. Zhang H, Yushkevich PA, Alexander DC, Gee JC (2006): Deformable registration of diffusion tensor MR images with explicit orientation optimization. *Med Image Anal*. 10: 764–85.
7. Tromp DPM, Williams LE, Fox AS, Oler JA, Roseboom PH, Rogers GM, *et al.* (2019): Altered uncinate fasciculus microstructure in childhood anxiety disorders in boys but not girls. *Am J Psychiatry*. 176: 208–216.
8. Basser PJ, Pajevic S, Pierpaoli C, Duda J, Aldroubi A (2000): In vivo fiber tractography using DT-MRI data. *Magn Reson Med*. 44: 625–632.
9. Lazar M, Weinstein DM, Tsuruda JS, Hasan KM, Arfanakis K, Meyerand ME, *et al.* (2003): White matter tractography using diffusion tensor deflection. *Hum Brain Mapp*. 18: 306–21.
10. Wang R, Benner T, Sorensen AG, Wedeen VJ (2007): Diffusion Toolkit : A Software Package for Diffusion Imaging Data Processing and Tractography. *Proc Intl Soc Mag Reson Med*. 15: 3720.
11. Mori S, Kaufmann WE, Davatzikos C, Stieltjes B, Amodei L, Fredericksen K, *et al.* (2002): Imaging Cortical Association Tracts in the Human Brain Using Diffusion-Tensor-Based Axonal Tracking. 223: 215–223.
12. Tromp D (2016): DTI Tutorial 3 - Fiber Tractography. *doi.org*. . doi: 10.15200/winn.146228.88526.

13. Tromp D (2016): The diffusion tensor, and its relation to FA, MD, AD and RD. *doi.org*.
. doi: 10.15200/winn.146119.94804.
14. Tromp D (2018): Calculate tract based weighted means. *Authorea Prepr*. 1–7.
15. Alexander AL, Hurley S a., Samsonov A a., Adluru N, Hosseinbor AP, Mossahebi P, *et al.* (2011): Characterization of cerebral white matter properties using quantitative magnetic resonance imaging stains. *Brain Connect*. 1: 423–46.